2015 IEEE International Conference on Robotics and Automation (ICRA)
Washington State Convention Center
Seattle, Washington, May 26-30, 2015

Flight Control Systems of a Quad Tilt Rotor Unmanned Aerial Vehicle for a Large Attitude Change

Atsushi Oosedo[1], Satoko Abiko[1], Shota Narasaki[1], Atsushi Kuno[1], Atsushi Konno[2] and Masaru Uchiyama[1]

***Abstract*— Quad tilt rotor Unmanned Aerial Vehicle (UAV) solves the problem of underacuated system in general quadrotor UAV. The quad tilt rotor UAV can control position and attitude independently by tilting directions of propellers. However, the flight control system in a wide range of attitudes has not been discussed yet, e.g. a UAV flying and hovering with a 90 [°] pitch angle and can flip over when the range of the tilting motor rotates wide enough. In this paper, we present the attitude transition flight control system for pitch angles ranging 0 [°] to 90 [°] since flight condition with a 90 [°] pitch angle significantly differs from that in a conventional quadrotor UAV flight, and then adequate control system and sufficient experimental validation are necessary for stable flight in a wide range of attitude conditions.**

I. INTRODUCTION

In recent years, unmanned aerial vehicles (UAVs) have been actively used in various fields. Among the various types of UAVs, quadrotor UAVs are being exploited in the fields of autonomous aerial photography and surveys because of their high attitude capability. The quadrotor UAVs generally move 6 degrees of freedom (DOF) with only 4 DOF control inputs, which means they are underactuated systems. Therefore, with this system configuration, only the altitude and 3 DOF attitude can be independently controlled, while the translation motion can be achieved by tilting the airframe for generating the horizontal component of propulsion. If quadrotor UAV had the capability of flying to an arbitrary position and attitude independently, they would realize the above mentioned tasks with higher performance and become even more widespread in various applications (for example, indoor flight where flight space is limited) [1][2].

To solve the above problem, several studies on multi-rotor UAVs with tilting propellers have been carried out. Ryll et al. developed a quadrotor UAV with 8 control inputs that allow for independent position and attitude control by tilting the propellers themselves instead of changing the attitude of the body. They employed linearized compensation control based on dynamics [3], and also succeeded in flight experiments; however, the range of the tilting angle was relatively narrow [4]. Segui-Gasco et al. developed a UAV with 12 actuators, of which 4 motors were used for propeller rotations and 8 servo motors were used for 2 degrees of freedom tilting motion in each propeller [5]. Although the proposed concept could arbitrarily determine the directions of propeller thrust, it required rather complex control calculations, and was difficult to use to achieve stable flight and led to frequent flight failure. Further, the tilting propeller mechanism also improves the yaw control performance [6].

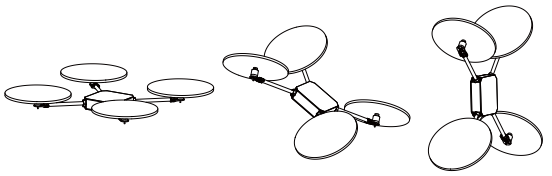

(a) Normal (Conventional) Flight (b) Tilted Flight (c) Perpendicularly-oriented Flight

Fig. 1. Independent position and attitude control by a quad tilt rotor UAV.

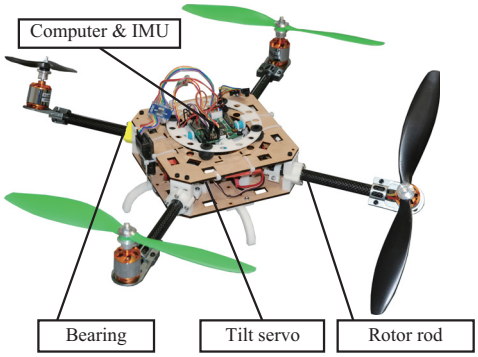

Fig. 2. The quad tilt rotor UAV developed.

Although the previous studies could achieve independent position and attitude control, the flight performance in wide range of attitude has not been discussed yet, e.g. the UAV flies and hovers with 90 [°] pitch angle (Fig. 1(c)) and even the UAV can flip over when the range of the tilting motor is wide enough. Such flight conditions allow the UAV to fly easier in narrow space or provide possibility to work on vertical wall surfaces etc.

In this paper, we focus on the attitude transition flight control system for pitch angles from 0 [°] to 90 [°] (perpendicularly-oriented flight, as shown in Fig. 1(c)) since the flight condition at a 90 [°] pitch angle significantly differs from that in a conventional quadrotor UAVs. An adequate control system and sufficient experimental validation are necessary for stable flight in a wide range of attitude conditions. Section II describes a developed quadrotor UAV with 4 tilting mechanisms for 4 propeller units. Section III explains dynamics modeling for the quad tilt rotor UAV.

[1]Department of Mechanical Systems and Design, Graduate School of Engineering, Tohoku University, 6-6-01 Aoba-yama, Sendai 980-8579, Japan { oosedo, abiko, narasaki, kuno, uchiyama } @space.mech.tohoku.ac.jp
[2]Division of System Science and Informatics, Hokkaido University, Kita 14, Nishi 9, Kita-ku, Sapporo, Hokkaido, 060-0814, Japan konno@ssi.ist.hokudai.ac.jp

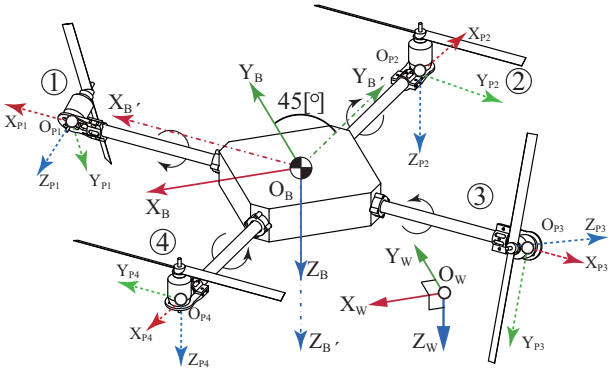

Fig. 3. Coordinate systems.

Section IV proposes control system with low calculation cost for on-board calculation on the basis of PID control. Section V shows simulation and experimental verification. Finally Section VI summarizes the conclusions.

II. Development of a Quad Tilt Rotor UAV

A. Fuselage

The developed UAV has 8 control inputs, four of which are used for the rotation of the propeller and four of which are used for the tilting motion for each propeller. Fig. 2 shows the quad tilt rotor UAV developed. It weigh 1.4 [kg], has a diameter of 0.45 [m] (without propellers), and a height of 0.25 [m]. The body frame of the UAV is constructed from a medium density fiberboard and each rotor rod is made of carbon fiber.

The tilt rotor mechanism is unique development. The rotor is tilted using of a radio-controlled servo (MD260, Hnege Co). The rotor rods radiate from the center of the body. Their root is mounted on the rotation axis of the tilt servo. Furthermore, each rotor rod is supported by a bearing. Hence, the tilting of the rotor is not restricted by the tilt rotor mechanism. The range of tilting angle is from 0 to 260 [°]. Each of the mounts for the servo, rod, and bearing are developed using 3D printer.

A fixed pitch propeller and brushless DC motor (D2836/8 1100kv, Turnigy Co) are used as propulsion units. The diameter of the propeller is 0.2794 [m] and the pitch is 0.11938 [m]. As a result, a thrust to weight ratio is 1.75.

B. Electronics

We developed a flight control board for the developed UAV. A commercially available microcomputer (RX62T, Renesas Technology) is used as the main computer, which calculates control inputs by using data from each sensor module and sends command signals to each motor. The maximum control outputs are 12 channels. The control frequency is 200 [Hz]. The developed board is equipped with a 9 DOF inertial measurement unit in a single chip (MPU 9150, InvenSense). Flight logs are recorded on a micro-SD card.

TABLE I
Nomenclature.

m	:	mass of the UAV
i	:	rotor number (i=1−4)
j	:	axis (j=x,y,z)
Σ_W	:	earth-fixed coordinate system
Σ_B	:	body-fixed coordinate system
Σ_{Pi}	:	propeller-fixed coordinate system
$\boldsymbol{O}_{W,B,P_i}$	:	origin of each coordinate systems
(u,v,w)	:	velocity with respect to Σ_B
(p,q,r)	:	angular velocity around each axis of Σ_B
Ω_i	:	propeller revolution speed of each rotor
T_i	:	thrust force of each motor
Q_i	:	torque of each motor
k_T	:	thrust constant
k_Q	:	torque constant
$I_{B_{jj}}$	:	principal moment of inertia of the UAV including rotors
$I_{P_{jj}}$	:	principal moment of inertia of the rotor
${}^B\boldsymbol{R}_A$	:	rotation matrix from A to B
$\boldsymbol{R}_{ref}$	:	rotation matrix of the reference attitude
$\boldsymbol{R}_{cur}$	:	rotation matrix of the current attitude
η	:	angle of rotation between Σ_B and $\Sigma_{B'}$
ω_j	:	attitude error of each axis of Σ_B
δ_j	:	attitude control value
C_1	:	conversion constant from the torque to the tilt angle
C_2	:	conversion constant from the force to the tilt angle
P_{W_j}	:	position of the UAV
$e_{W,B}$	:	position of error
F_{Wj}	:	force of each axis component in Σ_W
$K_{P,I,D}$	:	attitude and position PID control gains
$\tilde{}_{cur,ref}$	:	current and reference parameter

The position is obtained from a GPS receiver module (LEA-6H module, uBlox) in outside flight and is obtained from a motion capture system in indoor flight.

III. Dynamics Modeling

This section explains the dynamics model of the quad tilt rotor UAV. The symbols used in this paper are listed in Table. I.

A. Coordinate systems

Fig. 3 shows the coordinate systems defined in this paper. The term Σ_W defines the earth-fixed coordinate system (inertial coordinates), Σ_B defines the body-fixed coordinate system, and Σ_{P_i} ($i=1-4$) defines each rotor-fixed coordinate system. The earth-fixed coordinate system defines the X_W axis as true north, the Y_W axis as east, and the Z_W axis as perpendicular downward.

The rotation motion about the X_B, Y_B, and Z_B axes are defined as roll, pitch, and yaw and the rotation angle around each axis is denoted as ϕ, θ, and ψ, respectively. The coordinate system of the aircraft is consistent in every flight mode. The direction from motor to the center of gravity (COG) is rotated by 45 [°] around the Z_B axis with respect to Σ_B. Further, X_{P_i} is defined as the tilting actuation axis and Z_{P_i} is defined as the negative direction on the thrust axis. The i-th actuated tilting angle is defined as α_i.

Moreover, the auxiliary coordinate system $\Sigma_{B'}$ is defined. $\Sigma_{B'}$ is rotated by 45 [°] around the Z_B axis so that the $X_{B'}$ axis coincides with the direction from O_{P_3} to O_{P_1} and the $Y_{B'}$

TABLE II
CONTROL FORCE AND TORQUE.

		Normal condition	Perpendicular condition
Translation	X_W	: Horizontal component of thrust by tilt of rotors	: Horizontal component of thrust by tilt of all rotor
	Y_W	: Horizontal component of thrust by tilt of rotors	: Differential thrust between (1&3) and (2&4) rotors
	Z_W	: Total thrust	: Total thrust
Rotation	X_B	: Differential thrust between (1&2) and (3&4) rotors	: Generated torque by tilting rotor between (1&2) and (3&4) rotors
	Y_B	: Differential thrust between (1&4) and (2&3) rotors	: Generated torque by tilting rotor between (1&4) and (2&3) rotors
	Z_B	: Tilt of all rotor	: Differential thrust between (1&2) and (3&4) rotors

axis coincides with the direction from O_{P_4} to O_{P_2}. The $\Sigma_{B'}$ is used for calculating the offset tilt angle in Section. IV-C.

B. Dynamics Modeling

The equations of motion of the quad tilt rotor UAV are discussed in this sction . In the given equations, s_i and c_i are expressed as $s_i = \sin(\alpha_i)$, and $c_i = \cos(\alpha_i)$ respectively. The dynamic equations of the mathematical model in the aircraft body coordinates are expressed as follows:

- Translational dynamic equations

$$\begin{aligned} m(\dot{u} - rv + qw) &= \sin\eta(-T_1 s_1 - T_2 s_2 + T_3 s_3 \\ &\quad + T_4 s_4) - mg\sin(\theta). \quad (1) \\ m(\dot{v} - pw + ru) &= \sin\eta(T_1 s_1 - T_2 s_2 - T_3 s_3 \\ &\quad + T_4 s_4) + mg\sin(\phi)\cos(\theta). \quad (2) \\ m(\dot{w} - qu + pv) &= -\sum_{i=1}^{4} T_i c_i + mg\cos(\phi)\cos(\theta). \quad (3) \end{aligned}$$

- Rotational dynamic equations

$$\begin{aligned} I_{B_{xx}}\dot{p} &= (I_{B_{yy}} - I_{B_{zz}})qr - I_{P_{xx}}\sin\eta(\dot{\alpha}_2\Omega_2 c_2 - \dot{\alpha}_4\Omega_4 c_4) \\ &\quad + I_{P_{xx}}\sin\eta\left(q\sum_{i=1}^{4}(-1)^{i-1}\Omega_i c_i + r(\Omega_1 s_1 - \Omega_3 s_3)\right) \\ &\quad + \cos\eta(I_{P_{xx}}\ddot{\alpha}_1 - I_{P_{xx}}\ddot{\alpha}_3) + \sin\eta(I_{P_{xx}}\ddot{\alpha}_2 - I_{P_{xx}}\ddot{\alpha}_4) \\ &\quad + l\cos\eta(-T_1 c_1 - T_2 c_2 + T_3 c_3 + T_4 c_4) \\ &\quad + \cos\eta(Q_1 s_1 - Q_2 s_2 - Q_3 s_3 + Q_4 s_4). \quad (4) \\ I_{B_{yy}}\dot{q} &= (I_{B_{zz}} - I_{B_{xx}})pr - I_{P_{xx}}\sin\eta(\dot{\alpha}_1\Omega_1 c_1 - \dot{\alpha}_3\Omega_3 c_3) \\ &\quad - I_{P_{xx}}\sin\eta\left(p\sum_{i=1}^{4}(-1)^{i-1}\Omega_i c_i + r(\Omega_2 s_2 - \Omega_4 s_4)\right) \\ &\quad + \sin\eta(I_{P_{xx}}\ddot{\alpha}_1 - I_{P_{xx}}\ddot{\alpha}_3) + \cos\eta(I_{P_{xx}}\ddot{\alpha}_2 - I_{P_{xx}}\ddot{\alpha}_4) \\ &\quad + l\cos\eta(T_1 c_1 - T_2 c_2 - T_3 c_3 + T_4 c_4) \\ &\quad + \cos\eta(-Q_1 s_1 - Q_2 s_2 + Q_3 s_3 + Q_4 s_4). \quad (5) \\ I_{B_{zz}}\dot{r} &= (I_{B_{xx}} - I_{B_{yy}})pq + \sum_{i=1}^{4}\left(T_i s_i + (-1)^{i-1}Q_i c_i\right) \\ &\quad + I_{P_{xx}}(-p(\Omega_1 s_1 + \Omega_3 s_3) + q(\Omega_2 s_2 - \Omega_4 s_4)) \\ &\quad - I_{P_{xx}}\left(\sum_{i=1}^{4}(-1)^{i-1}\alpha_i\Omega_i s_i\right). \quad (6) \end{aligned}$$

The thrust and torque generated by a propeller are changed as a function of an airflow velocity into a propeller. However, assuming that the flight condition is extremely close to the state of hovering, the airflow velocity becomes 0 [m/s]. Hence, the change of airflow velocity is ignored in this study. Then the thrust and torque are defined as follows.

$$T_i \fallingdotseq k_T\Omega_i^2, \quad (7)$$

$$Q_i \fallingdotseq k_Q\Omega_i^2. \quad (8)$$

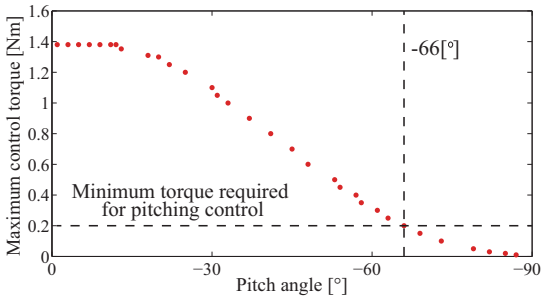

Fig. 4. Maximum pitch control torque.

IV. FLIGHT CONTROL SYSTEM

This section describes the flight control systems for different flight conditions and discusses a method for switching a control system with respect to the UAV attitude.

A. Concept of Control Design

A remarkable capability of the quad tilt rotor UAV is that it can hover at a wide range of attitudes by tilting its propeller units directly and can move in any directions without changing the attitude of the airframe itself. To achieve 6 DOF flight control, we determine "offset tilt angle" in control design. For example, when the pitch angle of the UAV is controlled to 0 [°], the offset tilt angle of Σ_{P_1} is determined as 0 [°], and the pitch angle of the UAV is driven to 90 [°], the offset tilt angle of Σ_{P_1} is determined as 90 [°]. The detailed calculation of the offset tilt angle is explained in Section. IV-C.

On the other hand, the change of the offset tilt angle leads to a decrease of attitude control torque that is generated by the thrust difference of the propellers. Fig. 4 shows the calculated maximum pitch control torque generated by the thrust difference between the rotors on Σ_{P_1} and Σ_{P_4} and the rotors on Σ_{P_2} and Σ_{P_3}. The figure shows that the maximum control torque decreases as the pitch angle of the UAV decreases. The developed UAV requires at least 0.2 [Nm] control torque for achieving stable flight. As a result, if the pitch angle is less than -66 [°], the pitch of the UAV cannot be controlled stably.

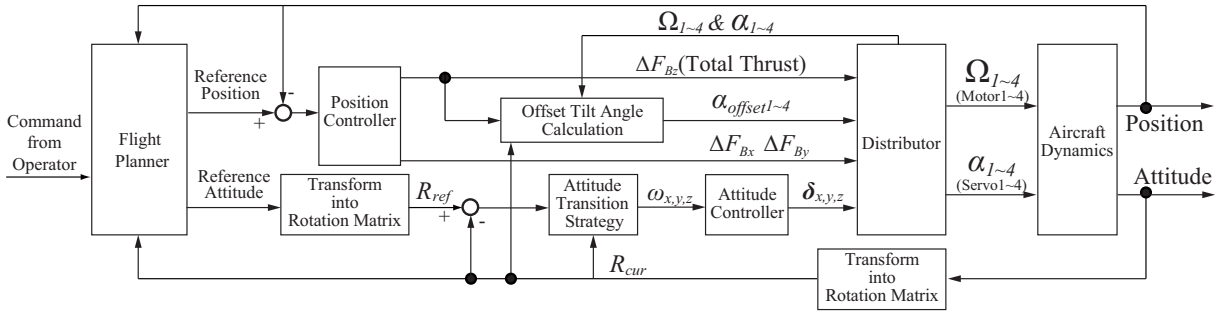

Fig. 5. Block diagram of the control system.

Therefore, two control systems with respect to the attitude of UAV are designed and these control systems are switched by the attitude change. In this paper, the flight when the pitch angle is between 0 and -66 [°] is defined as the normal condition and the flight when the pitch angle is between -66 and -90 [°] is defined as the perpendicular condition. Table. II lists the thrusts and torques used for translational and rotational motion in the two flight conditions. These control systems realize the independent position and attitude control in both flight conditions.

B. Control system

Fig. 5 shows a block diagram of the flight controller. The flight control system is designed based on a PID controller.

First, the UAV receives a command from an operator, the block labeled as "Flight Planner" generates the reference attitude and altitude from the prearranged flight plan and sensor information. $\boldsymbol{R}_{ref}$ and $\boldsymbol{R}_{cur}$ are sent to the block labeled as "Attitude Transition Strategy". This block calculates the errors around the X_B, Y_B, and Z_B axes of the aircraft body coordinates. In this paper, "Resolved Tilt-Twist Angle Feedback Control" [7] is used to calculate the attitude error for a high mobility aircraft. This method increases stability against large attitude disturbances. These errors, which are defined as ω_j $(j = x,y,z)$, are sent to the block labeled as "Attitude controller", where ω_j denote the minimum attitude error between the reference and current attitudes around the X_B, Y_B and Z_B axes, respectively. These desired quantities are expressed as follows:

$$\delta_j = \left(K_{P_1}\omega_j + K_{I_1}\int \omega_j dt + K_{D_1}\dot{\omega}_j \right) \qquad (j = x,y,z), \quad (9)$$

The block labeled as "Position Controller" calclates the position error in the earth-fixed coordinate sysytem, and $\boldsymbol{e}_W$ is translated to $\boldsymbol{e}_B$. The position controller generates the desired control forces $\Delta\boldsymbol{F}_B$. These desired quantities are given as follows:

$$\boldsymbol{e}_W = \boldsymbol{P}_{W_{ref}} - \boldsymbol{P}_{W_{cur}}, \quad (10)$$

$$\boldsymbol{e}_B = ({}^W\boldsymbol{R}_B)^T \boldsymbol{e}_W, \quad (11)$$

$$\begin{bmatrix} \Delta F_{B_x} \\ \Delta F_{B_y} \\ \Delta F_{B_z} \end{bmatrix} = K_{P_2}\boldsymbol{e}_B + K_{I_2}\int \boldsymbol{e}_B dt + K_{D_2}\dot{\boldsymbol{e}}_B + \begin{bmatrix} 0 \\ 0 \\ mg \end{bmatrix}, \quad (12)$$

These control torques and forces are sent to the block labeled as "Distributor". "Distributor" determines the reference tilt angle and the propeller revolution speed of each motor. The calculation of the distribution is presented in Section. IV-D.

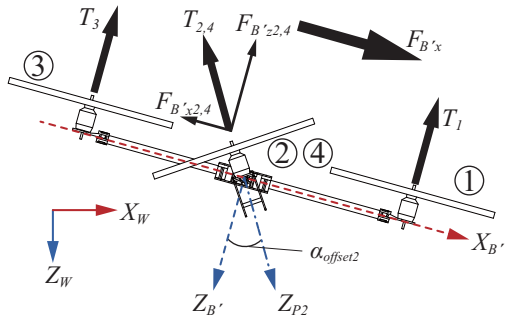

Fig. 6. Offset tilt angle.

C. Calculation of the offset tilt angle

Fig. 6 shows the concept of the calculation. This angle is necessary for stationary hovering with a constant attitude of the UAV. The calculation of the offset tilt angle is presented.

First, $\boldsymbol{F}_W$ is estimated from the current tilt angle and thrust. Second, in order to simplify the calculation, $\boldsymbol{F}_W$ is converted to $\boldsymbol{F}_{B'}$. Third, each offset tilt angle to cancel $F_{B'_{x,y}}$ is calculated. The horizontal component of the thrust produced by $\alpha_{offset1}$ and $\alpha_{offset3}$ cancel out $F_{B'_y}$ and that of the thrust produced by $\alpha_{offset2}$ and $\alpha_{offset4}$ cancels out $F_{B'_x}$. These offset tilt angles are expressed as follows:

$$\alpha_{offset1} = -\sin^{-1}\left(\frac{F_{B'_y} - F_{B'_{y3}}}{T_1}\right), \quad (13)$$

$$\alpha_{offset2} = \sin^{-1}\left(\frac{F_{B'_x} - F_{B'_{x4}}}{T_2}\right), \quad (14)$$

$$\alpha_{offset3} = \sin^{-1}\left(\frac{F_{B'_y} - F_{B'_{y1}}}{T_3}\right), \quad (15)$$

$$\alpha_{offset4} = -\sin^{-1}\left(\frac{F_{B'_x} - F_{B'_{x2}}}{T_4}\right), \quad (16)$$

where $F_{B'_{ji}}$ is the force of the j axis component of $\Sigma_{B'}$ produced by the i-th propeller. These offset tilt angles are sent to the distributor.

D. Distribution of the control parameters

"Distributor" determines the reference tilt angle and the propeller revolution speed of each motor. The reference

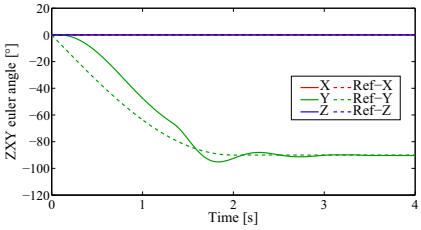

Fig. 7. Attitude of the first switching method.

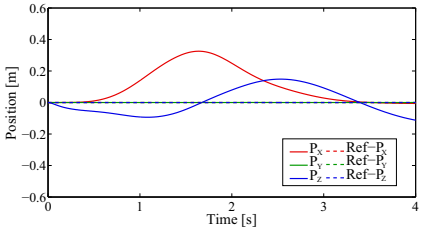

Fig. 8. Position of the first switching method.

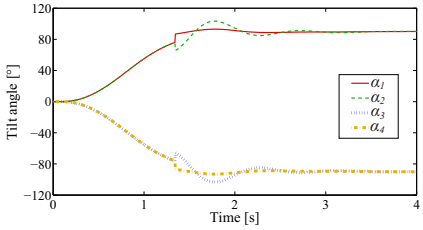

Fig. 9. Tilt angle of the first switching method.

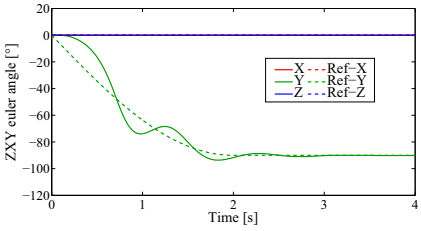

Fig. 10. Attitude of the second switching method.

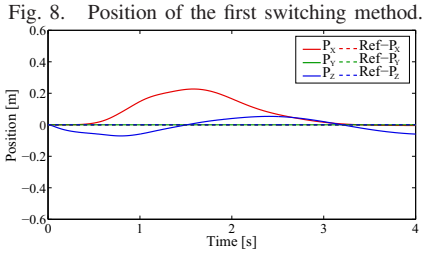

Fig. 11. Position of the second switching method.

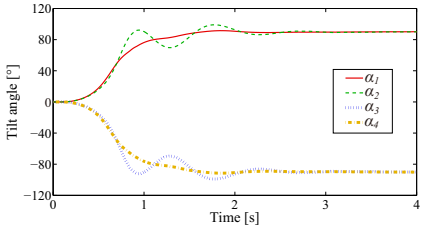

Fig. 12. Tilt angle of the second switching method.

propeller revolution speed and tilt angle of the rotors in the two conditions are given as

- Normal condition

$$\begin{bmatrix}\Omega_1^2\\ \Omega_2^2\\ \Omega_3^2\\ \Omega_4^2\end{bmatrix} = \frac{1}{4k_T k_Q}\begin{bmatrix}1 & 1 & -1\\ 1 & 1 & -1\\ 1 & -1 & 1\\ 1 & -1 & 1\end{bmatrix}\begin{bmatrix}k_Q\Delta F_{Bz}\\ k_T\delta_x\\ k_T\delta_y\end{bmatrix} \tag{17}$$

$$\begin{bmatrix}\alpha_1\\ \alpha_2\\ \alpha_3\\ \alpha_4\end{bmatrix} = \begin{bmatrix}\alpha_{offset1}\\ \alpha_{offset2}\\ \alpha_{offset3}\\ \alpha_{offset4}\end{bmatrix} + \frac{1}{4}\begin{bmatrix}-1 & -1 & 1\\ -1 & -1 & -1\\ -1 & 1 & -1\\ -1 & 1 & 1\end{bmatrix}\begin{bmatrix}C_1\delta_z\\ C_2\Delta F_{Bx}\\ C_2\Delta F_{By}\end{bmatrix} \tag{18}$$

- Perpendicular condition

$$\begin{bmatrix}\Omega_1^2\\ \Omega_2^2\\ \Omega_3^2\\ \Omega_4^2\end{bmatrix} = \frac{1}{4k_T k_Q}\begin{bmatrix}1 & 1 & -1\\ 1 & -1 & -1\\ 1 & 1 & 1\\ 1 & -1 & 1\end{bmatrix}\begin{bmatrix}k_Q\Delta F_{Bz}\\ k_Q\Delta F_{By}\\ k_T\delta_z\end{bmatrix} \tag{19}$$

$$\begin{bmatrix}\alpha_1\\ \alpha_2\\ \alpha_3\\ \alpha_4\end{bmatrix} = \begin{bmatrix}\alpha_{offset1}\\ \alpha_{offset2}\\ \alpha_{offset3}\\ \alpha_{offset4}\end{bmatrix} + \frac{1}{4}\begin{bmatrix}-1 & -1 & 1\\ -1 & -1 & -1\\ 1 & -1 & 1\\ 1 & -1 & -1\end{bmatrix}\begin{bmatrix}C_2\Delta F_{Bx}\\ C_1\delta_x\\ C_1\delta_y\end{bmatrix} \tag{20}$$

V. Verification

The designed systems for independent position and attitude control are validated by both simulations and experiments. In the verification, the pitch of UAV is continuously changed from $\theta = 0$ [°] to $\theta = -90$ [°].

When the attitude is drastically changed, the switching of the control systems in the two flight conditions becomes significant. This paper proposes two switching methods for flight control. The first switching method is the simplest way that the two control systems in two flight conditions are simply switched at $\theta = -66$ [°]. The second switching method is a composition of two control systems. If one control system has a shortage of control torque during a transition, the other control system compensates for the lack of control torque.

A. Simulational verification

The flight simulation is performed. A 3D flight simulator is developed using the technical computing language MATLAB R2012a (MathWorks, Inc.). The actuator delay and aerodynamic parameters are measured via experimentation, and the fuselage moment of inertia of the aircraft body coordinates is calculated by using 3D-CAD software (Solidworks2012).

Flight control systems for the normal condition and perpendicular condition and the two switching methods are implemented in the simulator. In the simulation, the reference pitch decreases from 0 to -90 [°] in 2 seconds. The reference roll and yaw is 0 [°], and the reference positions is 0 [m].

Figs. 7−12 show the attitude, position and tilt angle during simulation, respectively. Figs. 7 and 10 show that the attitude response of the first switching method is faster than that of the second switching method. Furthermore, attitude error of the second method is smaller than that of the first method. This distinction is due to the compensation of the control torque. Since the compensation improved the attitude control performance by about $\theta = -66$ [°], the attitude error decreases and the response accelerates. Moreover, Figs. 8 and 11 show that the improvement of attitude control performance decreases the position error.

Fig. 9 shows the tilt angle is changed rapidly at $\theta = -66$ [°]. This rapid change of the tilt angle occurs since the control system is switched from the normal condition to the perpendicular condition at $\theta = -66$ [°]. In contrast, Fig. 12 shows that the tilt angle in the second switching method changed smoothly.

These simulation results show that the designed independent control systems of position and attitude succeeded in 6 DOF flight control with two significantly different flight conditions. The compensation of control torque provides stabilization of the flight control.

B. Experimental verification

The designed 6 DOF flight control system for the two flight conditions and the second switching method are implemented on the developed UAV, and an indoor flight

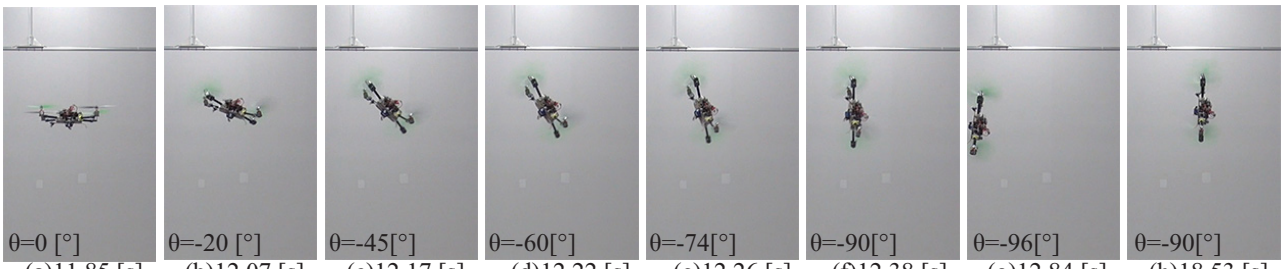

(a)11.85 [s] (b)12.07 [s] (c)12.17 [s] (d)12.22 [s] (e)12.26 [s] (f)12.38 [s] (g)12.84 [s] (h)18.53 [s]

Fig. 13. Snapshots of the transition to the perpendicular condition

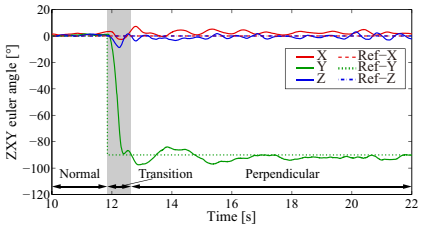

Fig. 14. Attitude during the experiment.

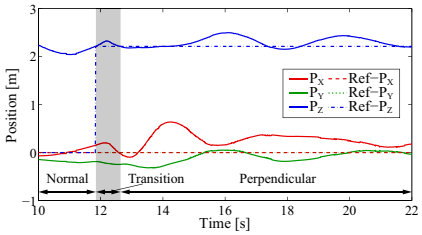

Fig. 15. Position during the experiment.

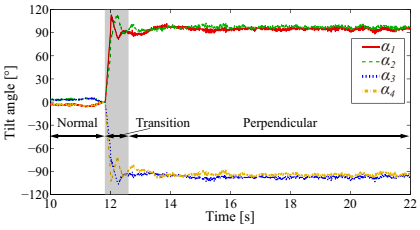

Fig. 16. Tilt angle during the experiment.

experiment was conducted. The UAV controls its attitude and position autonomously. After the UAV receives a command, the UAV commences an autonomous transition from the normal condition to the perpendicular condition.

Fig. 13 shows snapshots of the transition flight. The transition flight starts at experimental time t = 11.85 [s] and ends t = 12.38 [s]. Although the attitude of UAV changes rapidly, it is controlled stably during the experiment. Moreover, the UAV keep the constant altitude across the transition flight.

Figs. 14 and 16 show the attitude and the tilt angle during the experiment. Fig. 14 shows the pitch angle transits from $\theta = 0$ to -90 [°] in 0.53 seconds. The pitch angle decreasing of the experiment is faster than that of the simulation because the reference pitch angle is given as a step input. Therefore, there are overshoot about +6 [°]. After the transition, there are no large attitude errors during the flight. Fig 15 shows the position follows the reference throughout the experiment. The maximum position error is 0.5 [m] on the X_i axis. As it is clear from Fig. 16, to reduce position and position errors, tilt motors rotate large rotation right after the transition. Variation quantity of tilt angles get smaller with the decrease of these errors. Moreover, the tilt angle changes smoothly around $\theta = -66$ [°] because the switching method switched two control systems in an efficient way.

These experimental results show that the designed control systems succeeded in stable 6 DOF flight control with two significantly different flight conditions. The flight experiments verify the effectiveness of the transition procedure for achieving such conditions.

VI. Conclusions

This paper presented a development of the quad tilt rotor UAV and the verification of designed independent control systems for flight in wide range of attitude conditions. We developed a quad tilt rotor UAV which has 8 control inputs, of which 4 inputs control propeller revolutions and other 4 inputs tilt the directions. The developed UAV has a capability of wide range of tilting angle, namely 0 to 260 [°]. Therefore, control systems for significantly different attitude conditions were designed, e.g. normal and perpendicular conditions. Furthermore, two switching method for the flight control systems with respect to the attitude of UAV were proposed. These designed control systems and switching methods were implemented to the developed UAV, and the verification experiment was performed. These experimental results show that the designed control systems succeeded in stable 6 DOF flight control with two significantly different conditions. The flight experiments verified the effectiveness of the transition procedure for achieving such conditions.

In the future, we will challenge some missions considering features of a quad tilt rotor UAV will be conducted.

Acknowledgment

This work was supported by Grant-in-Aid for Japan society for the promotion of science fellows (25-4220).

References

[1] N. Michael et al., : “Collaborative mapping of an earthquake-damaged building via ground and aerial robots,” *Journal of Field Robotics*, vol. 29, Issue 5, pp.832-841, 2012.

[2] N. Metni, and T. Hamel, : “A UAV for bridge inspection: Visual servoing control law with orientation limits,” *Automation in Construction*, Vol. 17, Issue 1, pp.3-10, 2007.

[3] M. Ryll, H. H. Bulthoff, and P. Robuffo Giordano, : “Modeling and Control of a Quadrotor UAV with Tilting Propeller,” in *Proc. IEEE Int. Conf. on Robotics and Automation*, pp.4606-4613, 2012.

[4] M. Ryll, H. H. Bulthoff, and P. Robuffo Giordano, : “First Flight Tests for a Quadrotor UAV with Tilting Propeller,” in *Proc. IEEE Int. Conf. on Robotics and Automation*, pp.295-302, 2013.

[5] P. Segui-Gasco, Y. Al-Rihani, H. S. Shin, and A. Savvaris : “A Novel Actuation Concept for a Multi Rotor UAV,” *Journal of Intelligent & Robotic Systems*, Vol. 74, Issue 1-2, pp 173-191, 2014.

[6] S. King Phang, C. Cai, B. M Chen, and T. Heng Lee, : “Design and Mathematical Modeling of a 4-Standard-Propeller (4SP) Quadrotor,” in *Proc. 10th World Congress on Intelligent Control and Automation (WCICA)*, pp.3270 - 3275, 2012.

[7] T. Matsumoto, K. Kita, R. Suzuki, A. Oosedo, K. Go, Y. Hoshino, A.Konno and M. Uchiyama, : “A Hovering Control Strategy for a Tail-Sitter VTOL UAV that Increases Stability Against Large Disturbance”, in *Proc. IEEE Int. Conf. of Robotics and Automation*, pp.54-59, 2010.